Complete observational bounds on a fractal horizon holographic dark energy

Mariusz P. Dąbrowski[1, 2, 3, a] and Vincenzo Salzano[1, b]

[1] *Institute of Physics, University of Szczecin, Wielkopolska 15, 70-451 Szczecin, Poland*
[2] *National Centre for Nuclear Research, Andrzeja Sołtana 7, 05-400 Otwock, Poland*
[3] *Copernicus Center for Interdisciplinary Studies, Szczepańska 1/5, 31-011 Kraków, Poland*

(Dated: June 30, 2020)

A novel fractal structure for the cosmological horizon, inspired by COVID-19 geometry, which results in a modified area entropy, is applied to cosmology in order to serve dark energy. The constraints based on a complete set of observational data are derived. There is a strong Bayesian evidence in favor of such a dark energy in comparison to a standard ΛCDM model and that this energy cannot be reduced to a cosmological constant. Besides, there is a shift towards smaller values of baryon density parameter and towards larger values of the Hubble parameter, which reduces the Hubble tension.

Introduction. Black holes and cosmological horizons are very strongly explored phenomena in physics recently because they make the link between the classical and the quantum in the context of gravity. Through the Hawking temperature [1] and Bekenstein area entropy [2], they allow thermodynamics to be related to the classical geometry of space. So, any modification of geometry will influence the entropy related to the horizons. A modification of fractal nature has been recently proposed by Barrow [3] who was inspired by the COVID-19 virus geometrical structure. The idea is to consider the core sphere of the horizon with the attached number of heavily packed smaller spheres, to each of which some smaller spheres are latched on and so on, forming a fractal. Simple calculations which apply geometrical series allow to add up all the surfaces of such a hierarchical system. The resulting surface A_{eff} with an effective radius $r_{eff} = r^{1+\Delta/2}$ ($0 \leq \Delta \leq 1$) is larger than the core sphere surface A of radius r. The appropriate areas are $A_{eff} \propto r_{eff}^2$ and $A \propto r^2$ (so $r \propto A^{1/2}$). When $\Delta = 1$ one has the most intricate surface of the horizon with the COVID-19-like fractal geometry. Modification of the horizon area immediately leads to a change of the effective Bekenstein entropy, making it larger than in a smooth case, according to the formula

$$S_{eff} \propto A_{eff} \propto r_{eff}^2 \propto r^{2+\Delta} \propto A^{1+\frac{\Delta}{2}}, \tag{1}$$

where we can take as the smooth core sphere radius r either the black hole Schwarzschild radius r_s or the cosmological horizon length L. The exact formula in terms of the Planck area A_{Pl} is given by [3], $S_{eff} = k_B(A/A_{Pl})^{1+\Delta/2}$, where k_B is the Boltzmann constant.

In cosmology, there has been a vivid discussion of possible explanations of the dark energy phenomenon as contributed from cosmological horizons, leading to holographic dark energy [4]. It emerges that the fractal horizon can extra contribute to the matter. This has been first calculated in [5] and then tested in [6] using only few probes.

In this letter we apply the full set of cosmological data up-to-date to derive the most comprehensive bounds on the holographic and fractal parameters. The issue is that they strongly differ from the ones obtained in [5], as we will show later.

Theoretical background. According to [4] the holographic dark energy is given by $\rho_H \propto S_{eff} L^{-4}$ with the effective Bekenstein entropy $S_{eff} \propto A_{eff} \propto L^{2+\Delta}$, where L is the horizon length. Thus, following [5] we can express Barrow holographic dark energy (BH) as:

$$\rho_{BH} = \frac{3\,C^2}{8\pi G} L^{2\left(\frac{\Delta}{2}-1\right)}, \tag{2}$$

where C is the holographic parameter with dimensions of $[\mathsf{T}]^{-1}[\mathsf{L}]^{1-\Delta/2}$ and G the Newton gravitational constant. As suggested in [7], we identify the length L with the future event horizon:

$$L \equiv a \int_t^\infty \frac{dt'}{a} = a \int_a^\infty \frac{da'}{H(a')a'^2}, \tag{3}$$

where a is the scale factor. The cosmological equation is simply

$$H^2 = \frac{8\pi G}{3} \left(\rho_m + \rho_r + \rho_{BH}\right), \tag{4}$$

where the suffices m and r refer respectively to matter and radiation. Note that the standard continuity equation for matter and radiation is still valid, $\dot{\rho}_{m,r} + 3H(\rho_{m,r} + p_{m,r}/c^2) = 0$, where the pressure $p_i = w_i \rho_i$, with the equation of state parameter w_i being 0 for standard pressureless matter and 1/3 for radiation. We rewrite Eq. (4) as: $1 = \Omega_m(a) + \Omega_r(a) + \Omega_H(a)$, introducing the dimensionless density parameters $\Omega_i(a)$ [8], defined as $\Omega_{m,r}(a) = H_0^2/H^2(a)\Omega_{m,r}a^{-3(1+w_{m,r})}$ and

$$\Omega_{BH}(a) = \frac{C^2}{H^2(a)} L^{2\left(\frac{\Delta}{2}-1\right)}. \tag{5}$$

Combining previous equations one can express the Hubble parameter as

$$H(a) = H_0 \sqrt{\frac{\Omega_m a^{-3} + \Omega_r a^{-4}}{1 - \Omega_{BH}(a)}}. \tag{6}$$

In order to find the evolution of the holographic dark energy density, we follow [7] and [5] procedure: *(1.)* we insert Eq. (6) into Eq. (3); *(2.)* we obtain the future event horizon from inversion of Eq. (5); *(3.)* we compare results from step (1) and step (2) and differentiate both of them w.r.t. to a. We end up with the following differential equation for the BH dark energy (where prime is derivative with respect to a):

$$
\begin{aligned}
a\Omega_H'(a) = &\left(1+\frac{\Delta}{2}\right)\mathcal{F}_r(a) \\
&+ \Omega_H(a)\left(1-\Omega_H(a)\right)\left[\left(1+2\frac{\Delta}{2}\right)\mathcal{F}_m(a)\right. \\
&\left.+\ \left(1-\Omega_H(a)\right)^{\frac{\Delta/2}{2\left(\frac{\Delta}{2}-1\right)}}\Omega_H(a)^{\frac{1}{2\left(1-\frac{\Delta}{2}\right)}}\mathcal{Q}(a)\right],
\end{aligned}
\tag{7}
$$

with:

$$
\begin{aligned}
\mathcal{F}_r(a) &= -\frac{2\Omega_r a^{-4}}{\Omega_m a^{-3}+\Omega_r a^{-4}}, \\
\mathcal{F}_m(a) &= \frac{\Omega_m a^{-3}}{\Omega_m a^{-3}+\Omega_r a^{-4}}, \\
\mathcal{Q}(a) &= 2\left(1-\frac{\Delta}{2}\right)\left(H_0\sqrt{\Omega_m a^{-3}+\Omega_r a^{-4}}\right)^{\frac{\Delta/2}{1-\frac{\Delta}{2}}} C^{\frac{1}{\frac{\Delta}{2}-1}}.
\end{aligned}
\tag{8}
$$

It is easy to verify that in the limit $\Omega_r \to 0$ one retrieves Eq. (14) from [5].

Statistical Analysis. To analyze in full detail the compatibility of BH with cosmological data, we use the most updated set of data available today related to the geometrical global evolution of our Universe at large scales. We consider: Type Ia Supernovae (SNeIa) from the Pantheon sample; Cosmic Chronometers (CC); the gravitational lensing data from COSMOGRAIL's Wellspring project (H0LiCOW); the "Mayflower" sample of Gamma Ray Bursts (GRBs); Baryon Acoustic Oscillations (BAO) from several surveys; and the latest *Planck* 2018 release for Cosmic Microwave Background radiation (CMB).

We consider two different cases: the set which we call "full data", where we join both early- (CMB and BAO data from SDSS) and late-time observations (SNeIa, CC, H0LiCOW, GRBs and BAO data from WiggleZ); and the "late-time" data set, which includes only late-time data. We have decided to consider these two cases separately, because while on the one hand early-time data have much more stringent constraining power in cosmological model inference than late-time ones, on the other hand, they seem to be biased to statistically support a standard ΛCDM model, i.e. a cosmological constant as dark energy. By separating data in such a way, we could aim to have some more insight into a possible presence of a time varying dark energy candidate.

To perform our statistical analysis, we define the total χ^2 as the sum of all the contributions considered, $\chi^2 = \chi^2_{SN} + \chi^2_G + \chi^2_H + \chi^2_{HCOW} + \chi^2_{BAO} + \chi^2_{CMB}$. To minimize the χ^2 we use our own code implementation of a Monte Carlo Markov Chain (MCMC) [9–11] and we test its convergence using the method of [12]. Finally, we assess BH reliability using Bayesian Evidence, $\mathcal{E}$. Our reference model is the standard ΛCDM model, analyzed with the same set of data. Then, we calculate the Bayesian Evidence using the algorithm from [13]. To reduce its prior dependence [14] and avoid any misleading estimation, we have used the same uninformative flat priors on the parameters for each model while running our MCMC codes, on a sufficiently wide range, so that a further increasing has negligible impact on $\mathcal{E}$. Such priors are mainly physically motivated: $0 < \Omega_b < \Omega_m < 1$, $0 < h < 1$, $0 \leq \Delta \leq 1$ [3], and $C > 0$ (given Eq. 2, we cannot discriminate among positive and negative values). After the Bayesian Evidence, we define the Bayes Factor as the ratio of evidence between two models, M_i and M_j, $\mathcal{B}^i_j = \mathcal{E}_i/\mathcal{E}_j$: if $\mathcal{B}^i_j > 1$, model M_i is preferred over M_j, given the data. As stated above, here the ΛCDM model will play the role of the reference models M_j. Finally, in order to state how much better is model M_i with respect to model M_j, we have followed the Jeffreys' Scale [15].

Type Ia Supernovae. The Pantheon compilation [16] is made of 1048 objects spanning the redshift range $0.01 < z < 2.26$. The corresponding χ^2_{SN} is defined as $\chi^2_{SN} = \Delta\boldsymbol{\mu}^{SN} \cdot \mathbf{C}^{-1}_{SN} \cdot \Delta\boldsymbol{\mu}^{SN}$, where $\Delta\boldsymbol{\mu} = \mu_{\rm theo} - \mu_{\rm obs}$ is the difference between the theoretical and the observed value of the distance modulus for each SNeIa and $\mathbf{C}_{SN}$ the total covariance matrix. Note that we do not use the binned version as in [6], but the full one. The distance modulus is defined as $\mu(z,\boldsymbol{p}) = 5\log_{10}[d_L(z,\boldsymbol{p})] + \mu_0$, where the dimensionless luminosity distance $d_L(z,\boldsymbol{p}) = (1+z)d_M(z,\boldsymbol{p})$ with

$$
d_M(z,\boldsymbol{p}) = \int_0^z \frac{dz'}{E(z',\boldsymbol{p})} \tag{9}
$$

the dimensionless comoving distance and $\boldsymbol{\theta}$ the vector of cosmological parameters. Because of the degeneracy between the Hubble constant H_0 and the SNeIa absolute magnitude (both included in the nuisance parameter μ_0), we marginalize the χ^2_{SN} over μ_0 following [17], obtaining $\chi^2_{SN} = a + \log d/(2\pi) - b^2/d$, where $a \equiv (\Delta\boldsymbol{\mu}_{SN})^T \cdot \mathbf{C}^{-1}_{SN} \cdot \Delta\boldsymbol{\mu}_{SN}$, $b \equiv \left(\Delta\boldsymbol{\mu}^{SN}\right)^T \cdot \mathbf{C}^{-1}_{SN} \cdot \mathbf{1}$, $d \equiv \mathbf{1} \cdot \mathbf{C}^{-1}_{SN} \cdot \mathbf{1}$ and $\mathbf{1}$ is the identity matrix.

Cosmic Chronometers. The definition of CC is used for Early-Type galaxies which exhibit a passive evolution and a characteristic feature in their spectra [18], for which can be used as clocks and provide measurements of the Hubble parameter $H(z)$ [19]. The sample we are going to use in this work is from [20] and covers the redshift range $0 < z < 1.97$. The χ^2_H is defined as

$$
\chi^2_H = \sum_{i=1}^{24} \frac{\left(H(z_i,\boldsymbol{p}) - H_{obs}(z_i)\right)^2}{\sigma^2_H(z_i)}, \tag{10}
$$

where $\sigma_H(z_i)$ are the observational errors on the measured values $H_{obs}(z_i)$.

H0LiCOW. H0LiCOW [21] has used 6 selected lensed quasars [22] for which it was possible to retrieve multiple (lensing) images. When multiple images are produced, they can exhibit a time delay at collection given by

$$t(\boldsymbol{\theta},\boldsymbol{\beta}) = \frac{1+z_L}{c}\frac{D_L D_S}{D_{LS}}\left[\frac{1}{2}(\boldsymbol{\theta}-\boldsymbol{\beta})^2 - \hat{\Psi}(\boldsymbol{\theta})\right]. \quad (11)$$

In a typical gravitational lensing configuration [23], z_L is the lens redshift, $\boldsymbol{\theta}$ the angular position of the image, $\boldsymbol{\beta}$ the angular position of the source and $\hat{\Psi}$ the effective lens potential. The distances D_S, D_L and D_{LS} are, respectively, the angular diameter distances from the source to the observer, from the lens to the observer, and between source and lens. The angular diameter distance is given by $D_A(z,\boldsymbol{p}) = D_M(z,\boldsymbol{p})/(1+z)$, where the comoving distance is $D_M(z,\boldsymbol{p}) = c/H_0 d_M(z,\boldsymbol{p})$. Thus, we have: $D_S = D_A(z_S)$, $D_L = D_A(z_L)$, and $D_{LS} = 1/(1+z_S)\left[(1+z_S)D_S - (1+z_L)D_L\right]$ [24]. The combination of distances which appears in Eq. (11), $D_{\Delta t} \equiv (1+z_L)D_L D_S/D_{LS}$, is generally called time-delay distance and is constrained by H0LiCOW. The data ($D^{obs}_{\Delta t,i}$) and the corresponding errors ($\sigma_{D_{\Delta t,i}}$) on this quantity for each of the 6 considered quasars are provided in [22]. Eventually, the χ^2 for H0LiCOW data is

$$\chi^2_{HCOW} = \sum_{i=1}^{6}\frac{\left(D_{\Delta t,i}(\boldsymbol{p}) - D^{obs}_{\Delta t,i}\right)^2}{\sigma^2_{D_{\Delta t,i}}}, \quad (12)$$

Gamma Ray Bursts. Although the possibility to "standardize" GRBs is still on debate, we focus on the "Mayflower" sample, made of 79 GRBs in the redshift interval $1.44 < z < 8.1$ [25], because it has been calibrated with a robust cosmological model independent procedure. The observational probe related to GRBs observable is the distance modulus, so the same procedure used for SNeIa is also applied here. The χ^2_G is thus given by $\chi^2_{GRB} = a + \log d/(2\pi) - b^2/d$ as well, with $a \equiv \left(\Delta\boldsymbol{\mu}^G\right)^T \cdot \mathbf{C}_G^{-1} \cdot \Delta\boldsymbol{\mu}^G$, $b \equiv \left(\Delta\boldsymbol{\mu}^G\right)^T \cdot \mathbf{C}_G^{-1} \cdot \mathbf{1}$ and $d \equiv \mathbf{1} \cdot \mathbf{C}_G^{-1} \cdot \mathbf{1}$.

Baryon Acoustic Oscillations. For BAO we consider multiple data sets from different surveys. In general, the χ^2 defined as $\chi^2_{BAO} = \Delta\boldsymbol{\mathcal{F}}^{BAO} \cdot \mathbf{C}^{-1}_{BAO} \cdot \Delta\boldsymbol{\mathcal{F}}^{BAO}$, has observables $\mathcal{F}^{BAO}$ which change from survey to survey.

When we employ the data from the WiggleZ Dark Energy Survey (at redshifts 0.44, 0.6 and 0.73) [26], the relevant physical quantities are the acoustic parameter $A(z,\boldsymbol{p}) = 100\sqrt{\Omega_m h^2}D_V(z,\boldsymbol{p})/(c\,z)$, where $h = H_0/100$, and the Alcock-Paczynski distortion parameter $F(z,\boldsymbol{p}) = (1+z)D_A(z,\boldsymbol{p})\,H(z,\boldsymbol{p})/c$, where D_A is the angular diameter distance and $D_V(z,\boldsymbol{\theta}) = [(1+z)^2 D_A^2(z,\boldsymbol{\theta})\,cz/H(z,\boldsymbol{\theta})]^{1/3}$ is the geometric mean of the radial ($\propto H^{-1}$) and tangential (D_A) BAO modes. Note that this data set is independent of early-time evolution, thus it is included in the late-time data analysis.

We also consider data from multiple analysis of SDSS-III Baryon Oscillation Spectroscopic Survey (BOSS) observations. Each of the following data is used for the full data analysis but not for the late-time one.

In the DR12 analysis described in [27], the following quantities are given: $D_M(z,\boldsymbol{p})r_s^{fid}(z_d)/r_s(z_d,\boldsymbol{p})$ and $H(z)r_s(z_d,\boldsymbol{p})/r_s^{fid}(z_d)$, where the sound horizon evaluated at the dragging redshift is $r_s(z_d)$, while $r_s^{fid}(z_d)$ is the sound horizon calculated for a given fiducial cosmological model (in this case, it is 147.78 Mpc). The dragging redshift is estimated using the analytical approximation provided in [28]. Finally, the sound horizon is defined as:

$$r_s(z,\boldsymbol{p}) = \int_z^\infty \frac{c_s(z')}{H(z',\boldsymbol{p})}\mathrm{d}z', \quad (13)$$

with the sound speed $c_s(z) = c/\sqrt{3(1+\overline{R}_b\,(1+z)^{-1})}$, and the baryon-to-photon density ratio parameter $\overline{R}_b = 31500\Omega_b\,h^2\,(T_{CMB}/2.7)^{-4}$, with $T_{CMB} = 2.726$ K.

From the DR12 we also include measurements derived from the void-galaxy cross-correlation [29]: $D_A(z=0.57)/r_s(z_d) = 9.383 \pm 0.077$ and $H(z=0.57)r_s(z_d) = (14.05 \pm 0.14)10^3\,\mathrm{km\,s^{-1}}$.

From the extended Baryon Oscillation Spectroscopic Survey (eBOSS) we use the point $D_V(z=1.52) = 3843 \pm 147\,r_s(zd)/r_s^{fid}(z_d)$ Mpc [30]. Finally, we also take into account data from eBOSS DR14 obtained from the combination of the Quasar-Lyman α autocorrelation function [31] with the cross-correlation measurement [32]: $D_A(z=2.34)/r_s(z_d) = 36.98^{+1.26}_{-1.18}$ and $c/[H(z=2.34)r_s(z_d)] = 9.00^{+0.22}_{-0.22}$.

Cosmic Microwave Background. As CMB data we use the shift parameters defined in [33] and derived from the latest *Planck* 2018 data release [34]. The χ^2_{CMB} is defined as $\chi^2_{CMB} = \Delta\boldsymbol{\mathcal{F}}^{CMB} \cdot \mathbf{C}^{-1}_{CMB} \cdot \Delta\boldsymbol{\mathcal{F}}^{CMB}$, where the vector $\mathcal{F}^{CMB}$ is made of the quantities $R(\boldsymbol{p}) \equiv \sqrt{\Omega_m H_0^2}r(z_*,\boldsymbol{p})/c$, $l_a(\boldsymbol{p}) \equiv \pi r(z_*,\boldsymbol{p})/r_s(z_*,\boldsymbol{p})$ and $\Omega_b\,h^2$. Here $r_s(z_*)$ is the comoving sound horizon evaluated at the photon-decoupling redshift evaluated using the fitting formula from [35], while r is the comoving distance at decoupling, i.e. $r(z_*,\boldsymbol{p}) = D_M(z_*,\boldsymbol{p})$.

Discussion and Conclusion. We display constraints on cosmological parameters from our MCMC analysis in Table I, and the convergence test on MCMC runs in Table II. The posterior distributions for each parameter are shown in Fig. 1.

If we compare our analysis to the one in [6], we can definitely assess that late-time-only observations are unable to constrain BH dark energy parameters, with the fractal parameter Δ spanning the full range of validity, and the BH characteristic energy scale C being well defined (contrarily to what found in [6]), but with large errors. The addition of early-time data *is crucial*: both parameters' confidence levels are now highly narrowed, as can be seen in the left panel of Fig. 2. Note that the

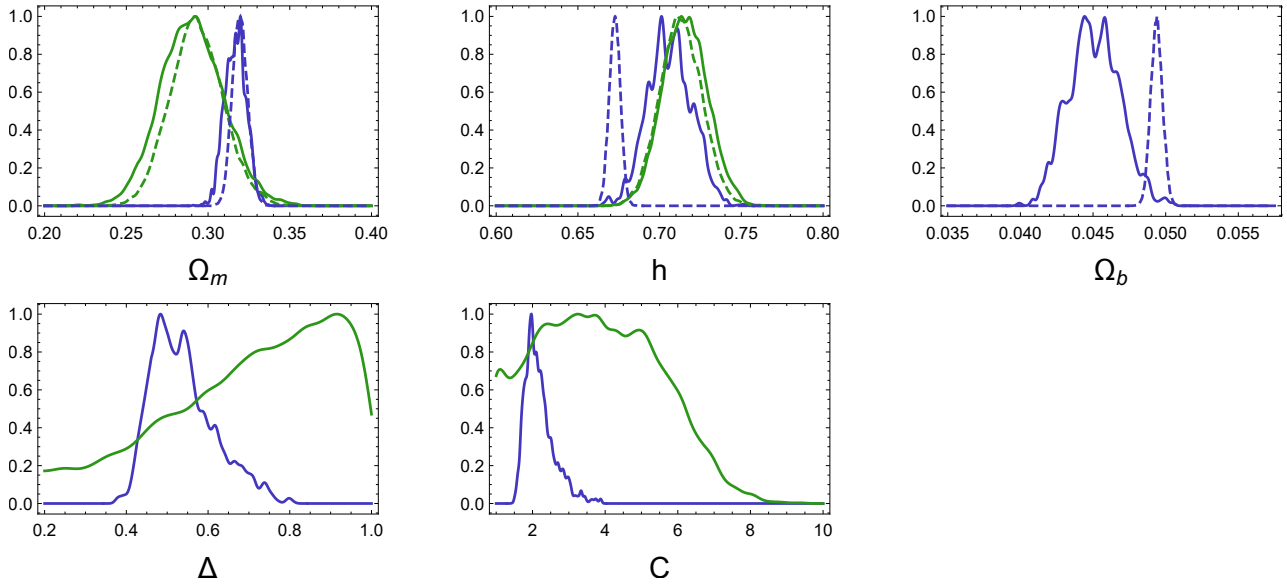

Figure 1. Normalized histograms for each cosmological parameter. In green: late-time analysis; in blue: full cosmological data set. Dashed: ΛCDM model; solid: Barrow Holographic dark energy.

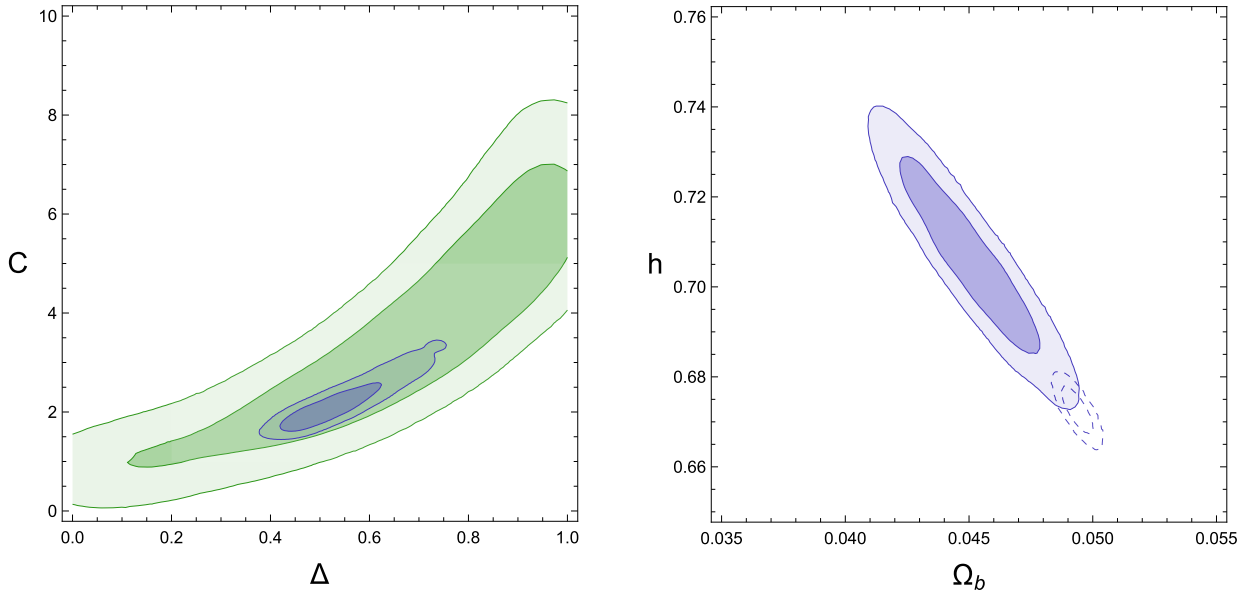

Figure 2. Joint contours for the Barrow Holographic dark energy parameters *(left panel)* and for the baryonic density parameter vs Hubble constant *(right panel)*. Colors as in previous figures. Hard colors: 68% confidence levels; soft colors: 95% confidence levels.

value of the fractal parameter Δ totally rejects both the lower ($\Delta = 0$) and the upper ($\Delta = 1$) limit.

The most striking result is given by the Bayes ratio: given Jeffreys' scale, there is "strong evidence", $\ln \mathcal{B}^i_j \approx 3.5$, in favour of BH dark energy w.r.t. a standard ΛCDM. This is a very surprising claim taking into account the outside of cosmological origin (i.e. COVID-19-like) nature of this type of dark energy, reinforced by the fact that the BH dark energy cannot be reduced to a cosmological constant.

Moreover, if we pay more attention to the values of the cosmological parameters, we can see that this statistical preference is led by a shift in both the Hubble constant, h, and the baryonic content, Ω_b (this is an important point, because Ω_b is called into question only when dealing with early-time data). As shown in the right panel of Fig. 2, we have a shift toward smaller values of Ω_b, partially consistent with the ΛCDM scenario on the upper tail,

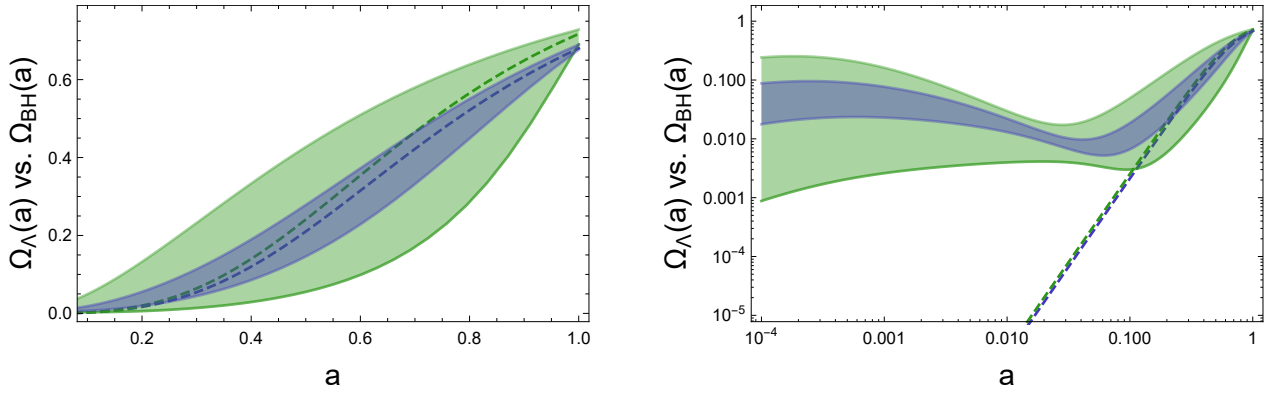

Figure 3. Evolution of dark energy at late times *(left panel)* and at early times *(right panel)*. Colors as in previous figures.

Table I. Results from MCMC analysis. We report 1σ confidence intervals for each parameter and the Bayes Factors.

	ΛCDM		BH	
	late	full	late	full
Ω_m	$0.293^{+0.016}_{-0.016}$	$0.319^{+0.005}_{-0.005}$	$0.290^{+0.019}_{-0.019}$	$0.317^{+0.007}_{-0.007}$
Ω_b	–	$0.0494^{+0.0004}_{-0.0004}$	–	$0.045^{+0.002}_{-0.002}$
h	$0.713^{+0.013}_{-0.013}$	$0.673^{+0.003}_{-0.003}$	$0.715^{+0.014}_{-0.013}$	$0.705^{+0.015}_{-0.015}$
Δ	–	–	> 0.60	$0.53^{+0.11}_{-0.07}$
C	–	–	$3.67^{+1.90}_{-1.79}$	$2.13^{+0.63}_{-0.30}$
$\mathcal{B}^i_j$	*1*	*1*	$0.48^{+0.05}_{-0.05}$	$32.604^{+0.001}_{-0.001}$
$\ln \mathcal{B}^i_j$	*0*	*0*	$-0.74^{+0.03}_{-0.03}$	$3.48^{+0.03}_{-0.04}$

Table II. Convergence test for MCMC. Convergence is achieved when all parameters have $j_* > 20$ and $r < 0.01$ [12].

	ΛCDM				BH			
	late		full		late		full	
	j_*	r	j_*	r	j_*	r	j_*	r
	(10^2)	(10^{-3})	(10^2)	(10^{-3})	(10^2)	(10^{-3})	(10^2)	(10^{-3})
Ω_m	70	0.2	230	0.2	4	0.6	2	2
Ω_b	–	–	10	0.2	–	–	0.8	3
h	10	0.2	10	0.2	10	0.4	1	3
Δ	–	–	–	–	0.7	2	0.8	3
C	–	–	–	–	12	1	0.4	5

and larger values of h, thus reducing the Hubble tension [36–38] to $\lesssim 2.75\sigma$. In Fig. 3 we additionally show how the BH dark energy differs from a standard cosmological constant mainly for early-times behaviour.

M.P.D. thanks John Barrow for the constructive feedback.

[a] mariusz.dabrowski@usz.edu.pl
[b] vincenzo.salzano@usz.edu.pl

[1] S. W. Hawking, Commun. Math. Phys. **43** (1975), 199-220
[2] J. D. Bekenstein, Phys. Rev. D **9** (1974), 3292-3300
[3] J. D. Barrow, [arXiv:2004.09444 [gr-qc]].
[4] S. Wang, Y. Wang and M. Li, Phys. Rept. **696** (2017), 1-57
[5] E. N. Saridakis, [arXiv:2005.04115 [gr-qc]].
[6] F. K. Anagnostopoulos, S. Basilakos and E. N. Saridakis, [arXiv:2005.10302 [gr-qc]].
[7] M. Li, Phys. Lett. B **603** (2004), 1
[8] We will follow the standard convention for which $\Omega_i(a)$, as a function, is the dimensionless density parameter at any scale factor a, while Ω_i, with no argument specified, will be the dimensionless density parameter at the present time, i.e. $\Omega_i(a=1) = \Omega_i$.
[9] B. A. Berg, *"Introduction to Markov chain Monte Carlo simulations and their statistical analysis"*, [arXiv:cond-mat/0410490 [cond-mat.stat-mech]].
[10] D. J. C. MacKay, *"Information Theory, Inference, and Learning Algorithms"*, Cambridge University Press (2003).
[11] R. M. Neal, *"Probabilistic Inference Using Markoc Chain Monte Carlo Methods"*, Technical Report CRG-TR-93-1, Department of Computer Science, University of Toronto (1993).
[12] J. Dunkley, M. Bucher, P. G. Ferreira, K. Moodley and C. Skordis, Mon. Not. Roy. Astron. Soc. **356** (2005), 925-936
[13] P. Mukherjee, D. Parkinson and A. R. Liddle, Astrophys. J. Lett. **638** (2006), L51-L54
[14] S. Nesseris and J. Garcia-Bellido, JCAP **08** (2013), 036
[15] H. Jeffreys, *"The Theory of Probability"*, Oxford Classic

Texts in the Physical Sciences (1939).
[16] D. M. Scolnic, D. O. Jones, A. Rest, Y. C. Pan, R. Chornock, R. J. Foley, M. E. Huber, R. Kessler, G. Narayan, A. G. Riess, S. Rodney, E. Berger, D. J. Brout, P. J. Challis, M. Drout, D. Finkbeiner, R. Lunnan, R. P. Kirshner, N. E. Sanders, E. Schlafly, S. Smartt, C. W. Stubbs, J. Tonry, W. M. Wood-Vasey, M. Foley, J. Hand, E. Johnson, W. S. Burgett, K. C. Chambers, P. W. Draper, K. W. Hodapp, N. Kaiser, R. P. Kudritzki, E. A. Magnier, N. Metcalfe, F. Bresolin, E. Gall, R. Kotak, M. McCrum and K. W. Smith, Astrophys. J. **859** (2018) no.2, 101
[17] A. Conley *et al.* [SNLS], Astrophys. J. Suppl. **192** (2011), 1
[18] R. Jimenez and A. Loeb, Astrophys. J. **573** (2002), 37-42
[19] M. Moresco, R. Jimenez, A. Cimatti and L. Pozzetti, JCAP **03** (2011), 045
[20] M. Moresco, Mon. Not. Roy. Astron. Soc. **450** (2015) no.1, L16-L20
[21] S. H. Suyu, V. Bonvin, F. Courbin, C. D. Fassnacht, C. E. Rusu, D. Sluse, T. Treu, K. C. Wong, M. W. Auger, X. Ding, S. Hilbert, P. J. Marshall, N. Rumbaugh, A. Sonnenfeld, M. Tewes, O. Tihhonova, A. Agnello, R. D. Blandford, G. C. F. Chen, T. Collett, L. V. E. Koopmans, K. Liao, G. Meylan and C. Spiniello, Mon. Not. Roy. Astron. Soc. **468** (2017) no.3, 2590-2604
[22] K. C. Wong, S. H. Suyu, G. C. F. Chen, C. E. Rusu, M. Millon, D. Sluse, V. Bonvin, C. D. Fassnacht, S. Taubenberger, M. W. Auger, S. Birrer, J. H. H. Chan, F. Courbin, S. Hilbert, O. Tihhonova, T. Treu, A. Agnello, X. Ding, I. Jee, E. Komatsu, A. J. Shajib, A. Sonnenfeld, R. D. Blandford, L. V. E. Koopmans, P. J. Marshall and G. Meylan, [arXiv:1907.04869 [astro-ph.CO]].
[23] P. Schneider, J. Ehlers and E. E. Falco, *"Gravitational Lenses*, Springer-Verlag Berlin Heidelberg New York (1992).
[24] D. W. Hogg, [arXiv:astro-ph/9905116 [astro-ph]].
[25] J. Liu and H. Wei, Gen. Rel. Grav. **47** (2015) no.11, 141
[26] C. Blake, S. Brough, M. Colless, C. Contreras, W. Couch, S. Croom, D. Croton, T. Davis, M. J. Drinkwater, K. Forster, D. Gilbank, M. Gladders, K. Glazebrook, B. Jelliffe, R. J. Jurek, I. h. Li, B. Madore, C. Martin, K. Pimbblet, G. B. Poole, M. Pracy, R. Sharp, E. Wisnioski, D. Woods, T. Wyder and H. Yee, Mon. Not. Roy. Astron. Soc. **425** (2012), 405-414
[27] S. Alam *et al.* [BOSS], Mon. Not. Roy. Astron. Soc. **470** (2017) no.3, 2617-2652
[28] D. J. Eisenstein and W. Hu, Astrophys. J. **496** (1998), 605
[29] S. Nadathur, P. M. Carter, W. J. Percival, H. A. Winther and J. Bautista, Phys. Rev. D **100** (2019) no.2, 023504
[30] M. Ata, F. Baumgarten, J. Bautista, F. Beutler, D. Bizyaev, M. R. Blanton, J. A. Blazek, A. S. Bolton, J. Brinkmann, J. R. Brownstein, E. Burtin, C. H. Chuang, J. Comparat, K. S. Dawson, A. de la Macorra, W. Du, H. du Mas des Bourboux, D. J. Eisenstein, H. Gil-Marin, K. Grabowski, J. Guy, N. Hand, S. Ho, T. A. Hutchinson, M. M. Ivanov, F. S. Kitaura, J. P. Kneib, P. Laurent, J. M. Le Goff, J. E. McEwen, E. M. Mueller, A. D. Myers, J. A. Newman, N. Palanque-Delabrouille, K. Pan, I. Paris, M. Pellejero-Ibanez, W. J. Percival, P. Petitjean, F. Prada, A. Prakash, S. A. Rodrguez-Torres, A. J. Ross, G. Rossi, R. Ruggeri, A. G. Sanchez, S. Satpathy, D. J. Schlegel, D. P. Schneider, H. J. Seo, A. Slosar, A. Streblyanska, J. L. Tinker, R. Tojeiro, M. Vargas Magana, M. Vivek, Y. Wang, C. Yeche, L. Yu, P. Zarrouk, C. Zhao, G. B. Zhao and F. Zhu, Mon. Not. Roy. Astron. Soc. **473** (2018) no.4, 4773-4794
[31] V. de Sainte Agathe, C. Balland, H. du Mas des Bourboux, N. G. Busca, M. Blomqvist, J. Guy, J. Rich, A. Font-Ribera, M. M. Pieri, J. E. Bautista, K. Dawson, J. M. Le Goff, A. de la Macorra, N. Palanque-Delabrouille, W. J. Percival, I. Prez-Rfols, D. P. Schneider, A. Slosar and C. Yche, Astron. Astrophys. **629** (2019), A85
[32] M. Blomqvist, H. du Mas des Bourboux, N. G. Busca, V. de Sainte Agathe, J. Rich, C. Balland, J. E. Bautista, K. Dawson, A. Font-Ribera, J. Guy, J. M. Le Goff, N. Palanque-Delabrouille, W. J. Percival, I. Prez-Rfols, M. M. Pieri, D. P. Schneider, A. Slosar and C. Yche, Astron. Astrophys. **629** (2019), A86
[33] Y. Wang and P. Mukherjee, Phys. Rev. D **76** (2007), 103533
[34] Z. Zhai and Y. Wang, JCAP **07** (2019), 005
[35] W. Hu and N. Sugiyama, Astrophys. J. **471** (1996), 542-570
[36] W. L. Freedman, Nature Astron. **1** (2017), 0121
[37] A. G. Riess, S. Casertano, W. Yuan, L. M. Macri and D. Scolnic, Astrophys. J. **876** (2019) no.1, 85
[38] A. G. Riess, Nature Rev. Phys. **2** (2019) no.1, 10-12